JOURNAL OF FLOOD ENGINEERING
Vol. 8 No. 1 (January-June, 2017)

Received: 15th September 2016 Revised: 10th October 2016 Accepted: 27th November 2016

REGRESSION METHOD FOR PREDICTING SNOW COVER IN CENTRAL ANDES IN ARGENTINA

Natalia K. Bisero[1] and Marcela H. González[2 3], Mariano H. Masiokas[4] and Saeid Eslamian[5]

[1]*National Weather Service, Argentina*
[2]*Department of Atmospheric Sciences FCEN University of Buenos Aires, Argentina*
[3]*Sea and Atmosphere Research Center, CIMA (CONICET-UBA), Argentina*
[4]*Argentine Institute of Snow Research, Glaciology and Environmental Sciences (IANIGLA CONICET), Argentina*
[5]*Department of Water Engineering, Isfahan University of Technology, Isfahan, Iran*

Abstract: The objective of this work is to find atmosphere circulation and sea surface temperature (SST) patterns, which are able to explain the snow precipitation in Central Andes, in Mendoza, and to develop a model for predicting snowfall over the region. For this purpose, a series of regional annual average snowfall (RAS) was used. In this case the series is representative for the Andes Mountain between 30° and 37°S, during 1951-2010. Masiokas *et al.* (2010] detailed the way this data set was constructed. Years were classified as "dry" if the annual value of snow was below the first quartile and "wet" if it exceeded the third quartile. The "wet" group was made up by 15 years, 9 years were Niño and 4 years were Niña, while the "dry" group was made up by 15 years, only 6 years were Niña and 3 were Niño. For each group, geopotential height anomalies at low levels (1000 Hpa, G1000), middle levels (500 Hpa, G500) and high levels (300 Hpa, G300), zonal wind (U) and meridional (V) at 850hPa and SST fields for different seasons (summer, spring, winter and autumn) were made. The method proposed for predicting snow precipitation in Central Andes (30°-37°S) in Argentina is a regression technique which uses atmosphere and oceanic predictors. The main conclusion is that an intensification (weakening) of the South Pacific anticyclone and the sub-polar low pressure systems and lower (higher) contribution moisture from the north, were observed in dry years (wet). This result let us select some variables and calculate the correlation field between them and RAS in order to define the best predictors. These predictors were used in a multiple regression model. A crossvalidation technique was applied to determine the forecast snow values. Some measures of efficiency were calculated to prove the agreement between predict and observed snow values.

Keywords: Central Andes, snow, seasonal forecast.

1. INTRODUCTION

Argentina is located in south-eastern South America. The Andes mountain extends all along the west of the country. It is important to distinguish the difference between low level circulation, east of the Andes, north and south of 38ºS. In the northern region, the Andes chain prevents the access of humidity from the Pacific Ocean, the flow is governed by the

South Atlantic High and as a consequence, winds prevail from the northeast. An intermittent low pressure system, originated by the combination of thermal and dynamical effects, is located between 20º and 30ºS, in a dry and relatively high area east of the Andes. This system is observed all year long, though it is deeper in summer than in winter. When this low is present, northerly flow is favored at low levels over the subtropical region. Therefore, the water vapor entering at low levels comes either from the tropical continent or from the Atlantic Ocean. In the first case, the easterly low-level flow at low latitudes is channeled towards the south between the Bolivian Plateau and the Brazilian Planalto, advecting warm and humid air to southern Brazil, Paraguay, Uruguay and subtropical Argentina and depicting a typical feature that many authors have studied (Lenters and Cook, 1995; Wang and Paegle, 1996; Barros *et al*, 2002 and Vera *et al* 2006). Often, in this flow there is an intense low-level jet that enhances humid and warm air advection from the Brazilian forest towards northern Argentina. Intermittent eruptions of polar fronts from the south modify this picture, causing a west or a southwest flow in low levels after the frontal passage. This happens with more frequency and greater displacement to the north in winter than in summer. The mean annual rainfall cycle is characterized by a minimum in winter and a maximum in summer.

South of 38ºS the Andes Mountain is lower and less solid so humid air arrives from the Pacific Ocean. The mean flow is from the west during all months in this region but it is stronger in winter. An intense contrast between the dense vegetation over the east part of the Andes Mountain and the dry plain that extends towards the Atlantic Ocean is one of the most enhanced features. In central Andes, south 36ºS, the annual rainfall cycle reverts and maximum precipitation takes place in winter. The interaction between the orography and mean flow determines that precipitation is greater in the proximity of the mountains meanwhile rainfall mainly decreases towards the Atlantic coast. Central Andes are located between 32º and 38ºS and its height decrease towards the south. The main humidity comes from the north especially in summer and so the annual rainfall cycle has a maximum in summer although heavy snow is present in high mountains in winter.

In that dry region the availability of drinking water is scarce and generally rivers provide the most important water quantity. The river runoff mostly depends on two factors: the actual rainfall and the snow accumulated in high mountains of the Andes. Anyway rainfall is low and the contribution of snowmelt to flow is of vital importance for the water supply of the region and to the development of numerous socio-economic activities. The snow in this part of the Andes is the main source of water for most of the rivers in the region, which is used for domestic consumption, irrigation, industry and electricity generation through dams (Masiokas *et al*. 2006). This is why it is important to know the climate variability as well as the ability to predict the availability of water, either in terms of water precipitation and snow melting. Therefore, it is necessary to increase the knowledge of climate variability of this region with the aim to improve the seasonal statistical forecast performance [Zareian and Eslamian, 2016].

2. METHODOLOGY

2.1. Statistical regression techniques to predict meteorological variables

Many authors have pointed out the difficulties still detected when forecasting seasonal climate (Barnston *et al*, 2005; Quan *et al*, 2006; among others). It is argued that because of the atmosphere´s internal variability, the seasonal predictability is inherently limited and there are some papers which deals with different methodologies to detect if seasonal prediction is more accurate than the simple climatology (Kumar, 2006; Coelho *et al*, 2005) and specially in South America an evaluation of seasonal climate forecast has been done (Goddard *et al*, 2003).

The possibility to improve the accuracy of seasonal precipitation forecast turns into an important matter and dynamic and statistical models have been used for that purpose. As the dynamical models have limited spatial resolution, in many cases, especially in small areas, statistical models became a relevant option for forecasting. The physical basis of seasonal climate predictability lies in the fact that slow variations in earth's boundary conditions (i.e. sea surface temperature or soil wetness) can influence atmospheric circulation and thus precipitation in far source region. This phenomenon is called teleconnections. The statistical forecasts are based on the detection of the relationships between rainfall and circulation and SST patterns that can be detected previously.

Different statistical techniques were used to determine these relationships in different regions of the world. For example, Gissila *et al* (2004) related sea surface temperatures with Ethiopian rainfall; Reason (2001) in South Africa and Zheng and Frederiksen (2006) in Australia using linear regression models where the predictand was rainfall and the predictors were different meteorological variables. Singhrattna *et al* (2005) developed two methods, a linear regression method and a polynomial-based non parametric method for forecasting Thailand summer monsoon rainfall. The last one showed significant skill especially during extreme cases. Gonzalez and Dominguez (2012) derived prediction schemes for standardized precipitation index in the Comahue region in Argentina, using multiple linear regressions and showed that 46% of its variability can be explained by this model. They derived a polynomial model too and it little improved the linear one, explaining the 49% of the variance. The multiple linear regression models consist in determine a function f:

$$y = f(x_1, x_2, x_3, \ldots, x_k) + e$$

where f is the fitting function of the predictors $x_1, x_2, x_3, \ldots, x_k$, y is the seasonal rainfall; and e is the error or residual assumed to be normally distributed with mean = 0 and variance = σ. The fitting functions (f) capture relationships locally.

The multiple linear regression models can be derived using a standard method or using the forward stepwise regression method (Wilks 1995), which retained only the variables, correlated with a 95% significance level. Forward stepwise regression is a model-building technique that finds subsets of predictor variables that most adequately predict responses

on a dependent variable by linear regression, given the specified criteria for adequacy of model fit (Darlington, 1990). The basic procedures involve identifying an initial model, repeatedly altering the model at the previous step by adding a predictor variable following a fixed criterion, and terminating the search when stepping is no longer possible as to the criteria. Predictors available to carry out the regression scheme were carefully selected, based on statistical significance and physical reasoning. Generally some models are used and a more efficient ensemble forecast is then obtained.

2.2. Description of climate forcings which influence snow precipitation in this region

A warming or cooling of some region of the oceans can act as a remote forcing generating teleconnections. The most relevant sea surface temperature pattern in the Pacific Ocean is the El Niño-Southern Oscillation (ENSO). The SST anomalies in tropical Pacific generate a Rossby wavepattern which propagates meridionally towards the middle-latitudes from the tropical source (Ropelewski and Halpert, 1987; Kidson, 1999; Nogues Paegle and Mo, 2002) and define a pattern, called the "Pacific South American Pattern". In South America, some authors have investigated these relations, for example, Compagnucci and Vargas (1998) showed that winters that precede a mature phase of El Niño (La Niña) were characterized by larger (smaller) amounts of snow over the Andes, north of 36ºS, which contributed to increase (decrease) the water volume of the rivers. Grimm *et al* (2002) detected specific patterns associated with both ENSO phases. Schneider and Gies (2004) found that rainfall decreased about 15% during strong warm phase of ENSO in the Andes Mountains, between 45ºS and 55ºS. Aceituno (1988) and Aceituno and Garreaud (1995) showed that that winter precipitation was greater than normal in Central Chile during negative phases of the Southern Oscillation Index (SOI), meanwhile Rutland and Fuenzalida (1991) and Montecinos and Aceituno (2003) observed a greater number of blocking events over the South Pacific during warm ENSO events.

Although ENSO is the most important remote forcing, without a doubt, the variability originated by other regional or remote sources cannot be disregarded. The Indian Ocean Dipole (IOD) is defined using SST (Saji *et al*, 2004); a positive IOD period is characterized by cooler than normal water in the tropical eastern Indian Ocean and warmer than normal water in the tropical western Indian Ocean. This pattern is associated with decreased rainfall in central and southern Australia. Chan *et al* (2008) showed that IOD is related to a dipolar pattern in rainfall anomalies between subtropical La Plata basin and central Brazil in South America, with reduced (enhanced) rainfall over the latter (former) during austral spring. Similarly to ENSO, it is also associated with a Rossby wave pattern extending from the subtropical south Indian Ocean to the subtropical South Atlantic. Gonzalez and Vera (2010), Gonzalez *et al* (2010) and Gonzalez and Cariaga (2011) studied the Comahue region, located in northwestern Patagonia, where there are located most of the energy resources of Argentina, and detected a strong relation between winter rainfall and IOD. Compagnucci and Araneo (2005) observed that variations in the Pacific Ocean surface that were not associated with ENSO, influence the interannual variability of river discharges along the Andes. Gonzalez

and Flores (2008) showed negative correlations between winter rainfall in the Andes Mountain range in Central Argentina and sea surface temperature in the tropical Indian Ocean.

Another teleconnection that influences rainfall in Central Andes is the Antarctic Oscillation, an annular-like pattern called "Southern Annular Mode" (SAM) (Thompson and Wallace, 2000) which is associated with the intensity of the sub-tropical high and sub-polar low belts and thus with the westerlies intensity over the Pacific Ocean. The positive phase of the SAM is defined by negative pressure anomalies at high latitudes (higher than 65ºS) combined with wave-like pattern in the middle-latitudes. When westerlies intensity increases, heat exchange between poles and mid-latitudes decreases and storm tracks have less meridional displacement. In South America some authors have analyzed this phenomenon: Silvestri and Vera (2003) found relation between SAM and rainfall amount in northeastern Argentina and southern Brazil particularly in late spring, Reboita *et al* (2009) detected a decrease of frontal activity when SAM is in a positive phase in the same area. Recently, Gonzalez (2013) and Gonzalez and Herrera (2014), Scarpati *et al* (2014) investigated rainfall and circulation connection and showed that cyclonic anomalies over the surrounding Atlantic and Pacific Oceans and over the continent enhance precipitation all over Patagonia in all seasons. Aravena and Luckman (2008) also detected relation between rainfall in Patagonia and circulation modes like ENSO and Antarctic Oscillation. These findings are consistent with the results detected in other parts of the world: Zheng and Frederiksen (2006) showed that the SAM affects summer rainfall New Zealand and Reason and Rouault (2005) showed wetter winters in western South Africa during negative SAM phase.

The joint action of the position of Atlantic and Pacific Highs and the SST anomalies in close proximity to the continent is another precipitation forcing. When SST is high, evaporation over the ocean is enhanced and moist onshore winds became intensified generating higher precipitation.

3. RESULTS AND DISCUSSION

3.1. Atmospheric and oceanic patterns related to wet and dry years.

In this section, the observed differences in the meteorological variables fields and SST between years with large and small amount of snow are analyzed. For this, a series of regional average annual flow and snow, in Andes between 30° and 37°S for the period 1951-2010 was used. The manner in which this data set is explained in detail in Masiokas *et al* (2006) was built. Seventeen stations located on both sides of the Central Andes belonging to Chilean institutions (Water Directorate) and Argentine (General Department of Irrigation in Mendoza, Secretariat of Water Resources of Argentina), with altitudes ranging between 500 and 3,500 m, were used to develop series of regional average flows and snow (Masiokas *et al*, 2006 and 2010). This area is characterized by precipitation, especially in the form of snow during winter, that decreases substantially in summer with the associated melting snow that contributes to the river flow.

Annual data flow and snow used in this work are Regional Average Flow (RAF) and Regional Average Snow (RAS), covering the periods 1909-2009 and 1951-2010, respectively. RAF data are calculated using the monthly average values from July to June of the following year (hydrological year), where each year is identified by the first months. The RAS series was built as follows: for each station maximum accumulated snow values of each winter were registered and the "maximum snow water equivalent" (MSWE) was obtained for each year as a substitute for total snow accumulation (Masiokas *et al*, 2006). This series is assigned the same hydrological year RAF, but the data relate only to the winter snow as they are the values of maximum accumulation between July and October. Regional averages for each year were calculated with data from selected stations (up to 8 stations). All values are expressed as a percentage of average common period 1951-2000 (for details see Masiokas *et al*, 2006 and 2010).

Figure 1 shows RAF and RAS series and also the first and third RAS quartile of the RAS, which functioned as cutoff values to characterize groups of dry and wet years. They were classified as "dry" years those where the annual value of snow is below the first quartile and years "wet" those where the annual snow exceeds the third quartile. RAF and

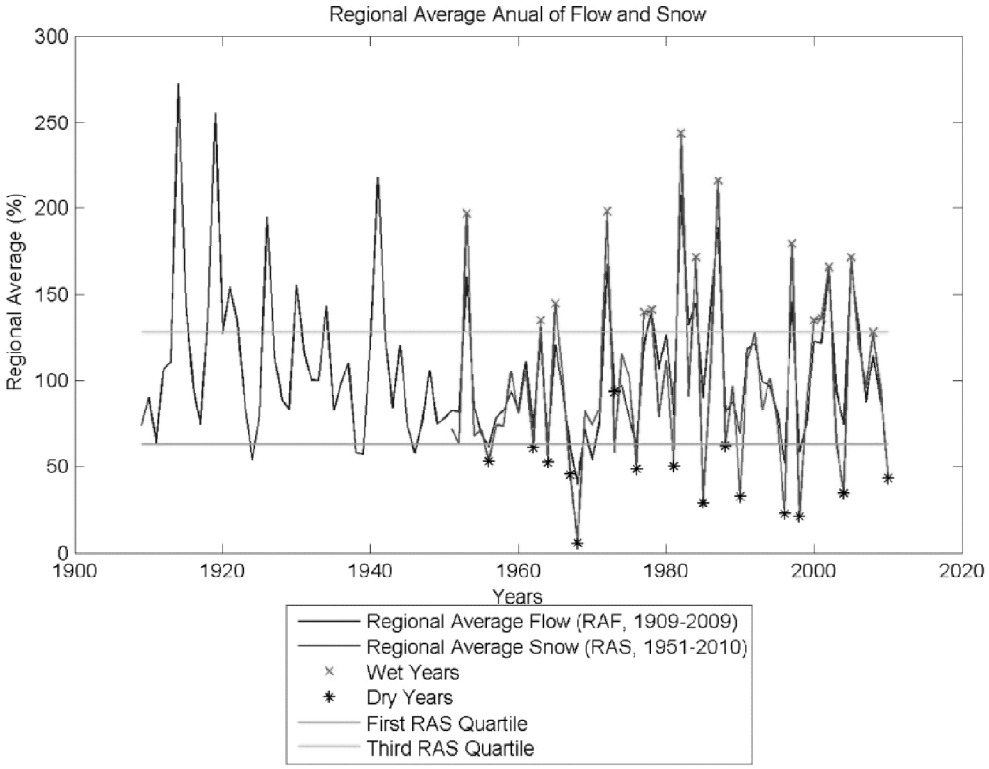

Figure 1: Regional Average Flow (RAF, blue line), Regional Average Snow (RAS, red line), wet years (AH, cross), Dry years (AS, asterik), First RAS quartile (green) and fouth RAS quartile (light blue)

RAS statistics as the mean, standard deviation, maximum and minimum values and percentiles were calculated. The main statistics of both series can be seen in Table 1. Table 2 shows the years as they were classified by this method. Firstly, it can be seen that the RAF and RAS series show a similar behavior. In fact the correlation between them is +0.921, significant at the 95% confidence level using a t-Student test. This indicates that the amount of snow represents well the observed annual flow in the river and they are acting as suppliers of the scarce water resources in the region.

Table 1
Statistics for RAF and RAS (%)

	Period	*Average*	*Standard Deviation*	*Maximum*	*Minimum*	*First Quartile*	*Third Quartile*
RAF	1909 – 2009	105,9	42,1	40,2	271,7	77,8	124,8
RAS	1951 - 2010	97,3	50,4	243,7	5,6	62,9	127,9

Table 2
Wet and dry years. Blue values are Niño years and red values are Niña years

Dry Years	*1956*	*1962*	*1964*	*1967*	*1968*	*1973*	*1976*	*1981*
	1985	**1988**	1990	1996	**1998**	**2004**	**2010**	
Wet Years	**1953**	**1963**	**1965**	**1972**	**1977**	1978	**1982**	**1984**
	1987	**1997**	**2000**	2001	**2002**	**2005**	**2008**	

Another observation is that 9 of the 15 years of wet group were Niño years and 4 of the 15 were Niña; meanwhile 6 of the 15 years of dry group were Niña and only 3 Niños (as classified by Jan Null, CCM, 2004, http://ggweather.com/enso/oni.htm). This indicates that in general, in the region studied, the (dry) wet years are associated with the warm (cold) phase of ENSO (Montecinos and Aceituno, 2003; Rutllan and Fuenzalida, 1991; Compagnucci and Vargas, 1998; Vera *et al*, 2006; among others).

The linear trend was calculated using a linear fit with the least squares method and the Student t-test was used to determinate significance. RAS linear trend was not significant with 95% confidence as the correlation coefficient was 0.1, indicating that snow records have not experienced a significant long-term trend during 1951-2010.

Significant cycles were obtained by applying the Blackman-Tukey spectral analysis methodology (Mitchell *et al*, 1971) using a Hamming window. The application of spectral analysis (Figure 2) showed that significant cycles with 90% but not significant with 95% confidence, are present in RAS series. The relevant cycles were those with 5/6 years and 30 months periods. A more detailed study was conducted by Compagnucci and Blanco (2000), who detected significant peaks between 4 and 7 years and 20 years when studying Atuel River flow in Mendoza.

Composites of geopotential height anomalies at low (1000 Hpa, G1000), middle (500 Hpa, G500) and high (300 Hpa, G300) levels, zonal (U) and meridional (V) 850 Hpa wind,

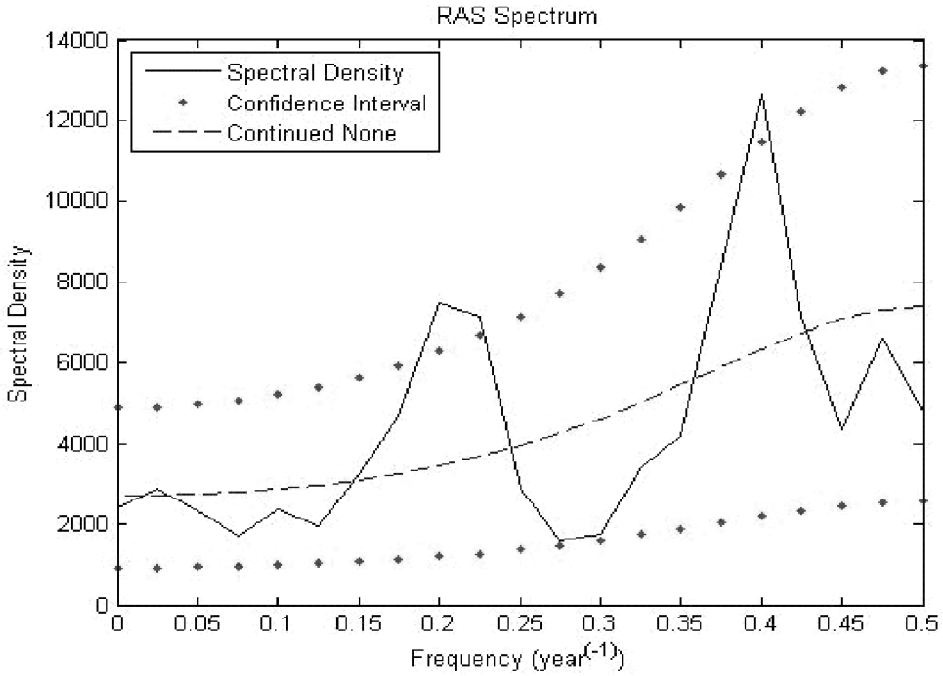

Figure 2: Spectral analysis of RAS. Frequencies are expressed in year-1. A Hamming window was used and the significance is 90%

precipitable water throughout the atmospheric column (PW) and SST for each of the seasons were computed for the two groups. The summer (December to February) and autumn (March to May) considered are previous and winter (June to August) and spring (September to November) are simultaneous to the hydrological cycle. Behavior differences in both cases (wet and dry) are analyzed. These data were obtained from the NCEP / NCAR (Kalnay *et al*, 1996).

G1000, G500 and G300 composites show intensified subpolar low and subtropical high in the eastern South Pacific in dry years, while in wet years, the opposite is true, weaken the subpolar low and subtropical high. This signal is hinted in autumn (March-April-May, figure not shown) and has its maximum signal in winter (June-July-August). Figure 3 shows both G1000 composites for winter. A dipole with a positive nucleus around 60° and a negative 30°S in the South Pacific, which reflects the weakening of the systems, can be observed in the wet years composite. The opposite situation occurs in the field of dry years composite. The same pattern is observed in G500 and G300 (figures not shown) with almost equal intensity. These patterns show that in wet years the weakening of the systems associated with a negative SAM phase, allows greater exchange between latitudes trajectories generating systems further north and more meridional component than in dry years. Other authors also detected this signal (Masiokas *et al*, 2006; Rutland and Fuenzalida, 1991).

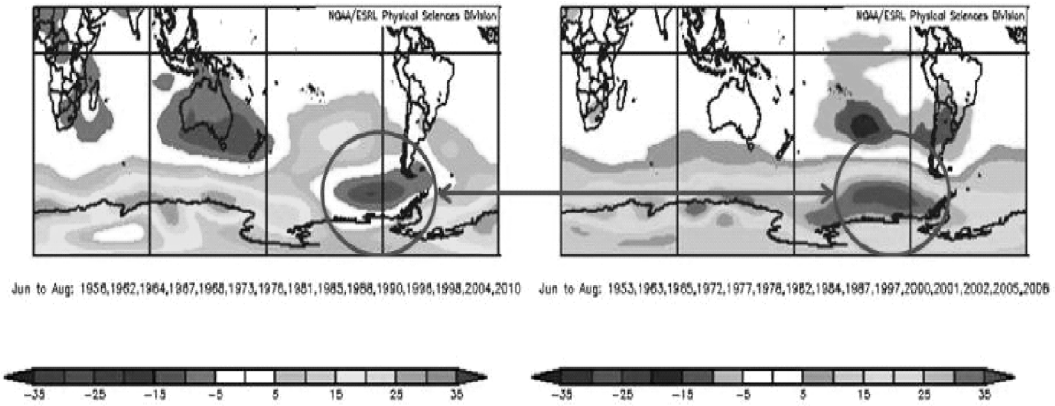

Figure 3: G1000 anomalies in June-July-August for dry years (left panel) and wet years (right panel)

The same effect is also reflected in the U composites, where an strengthening (weakenig) of westerlies is observed in dry (wet) years (Figure 4 for winter) that manifests itself as a positive (negative) center around 45°S in the South Pacific in dry (wet) years composite. This change in the magnitude of the wind zone is associated with the change in the intensity of the above described systems. The weakening of the subpolar low and subtropical high in the case of wet years, involving a less intense zonal flow more easily allows frontal systems can access the continent from the southwest. This pattern is then associated with a higher possibility of precipitation, which determines the condition of years classified as wet. These features are associated with a pattern of Antarctic Oscillation (SAM, Thompson and Wallace, 2000). Several authors have found that influences on precipitation in southern South America in the subtropical region (Silvestri and Vera, 2003; Gillett *et al*, 2006; Reboita *et al*, 2009). Indeed, G300 composite, in a polar stereographic projection in the southern hemisphere, allow to observe strong evidence of the negative phase of SAM associated with wet years in autumn (Figure 5) and lower signal in winter (Figure 6). It should be noted that the pattern of positive phase of SAM is not so clear in dry years.

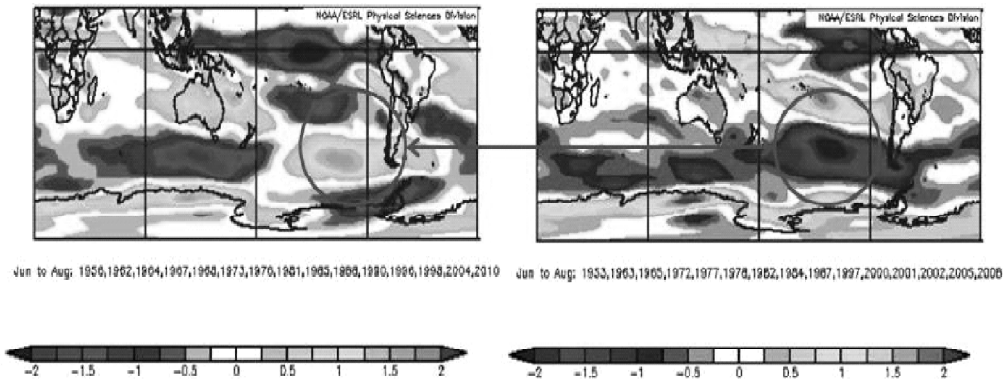

Figure 4: U850 anomalies in June-July-August for dry years (left panel) and wet years (right panel)

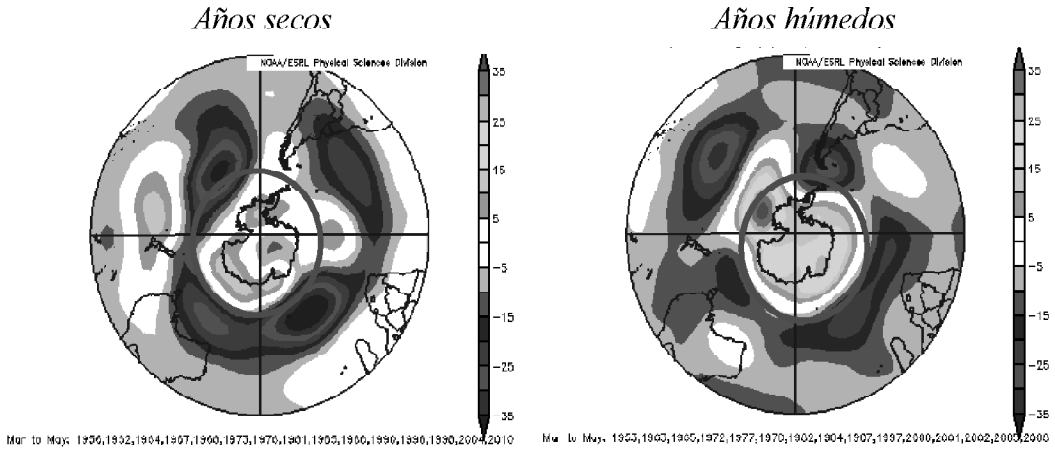

Figure 5: G300 anomalies in March-April-May for dry years (left panel) and wet years (right panel)

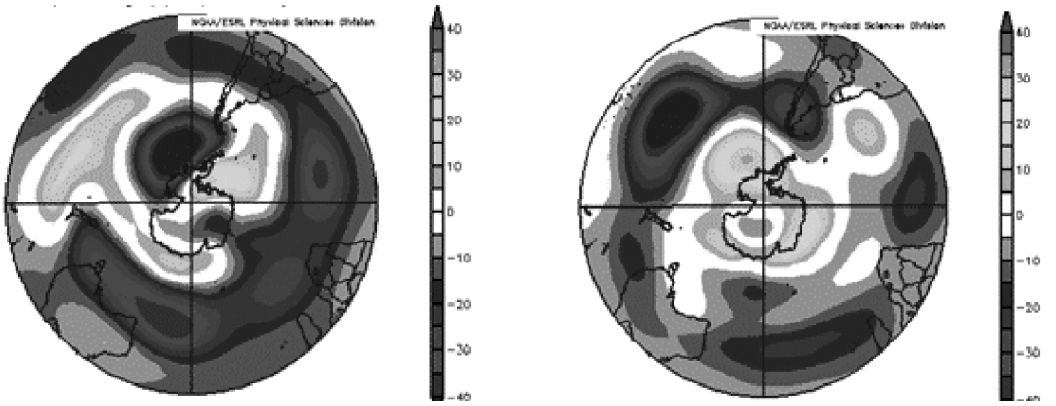

Figure 6: G300 anomalies in June-July-August for dry years (left panel) and wet years (right panel)

These results agree with that obtained by Masiokas *et al* (2006). They characterized two groups with the 10 driest years and the 10 wettest years of the series and detected a relationship between winter snow and atmospheric circulation. The pattern corresponding to the 10 wettest years showed a deadlock in the Subtropical Pacific and the weakening of the anticyclone, which determines more snow than normal on the study area, as shown in previous studies (Rutlland and Fuenzalida, 1991; Montecinos and Aceituno, 2003). For the 10 driest years the pattern is exactly the opposite. Also, on New Zealand and South Africa are highlighted positive and negative anomalies over the Southern Ocean. Other authors also showed the relationship with circulation such as Araneo (2006) and Araneo and Compagnucci (2008).

Differences in meridional low level (V) were also observed. There was a supply of moisture from the north (see negative anomaly over Central Andes in Figure 7) in wet

years while V anomalies are from the south (positive anomaly over Central Andes) in dry years, especially in winter (Figure 7) and spring (figure not shown). PW fields show no significant difference between the wet and dry years, unless the region with positive anomalies in central Argentina is more widespread in the case of wet years (Figure 8) cases. These positive anomalies of PW added to the northern V anomalies in winter collaborate in the production of higher rainfall in wet years.

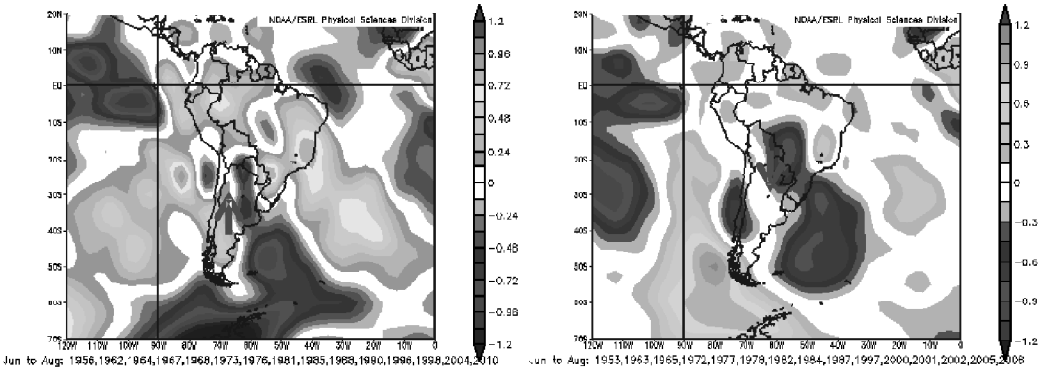

Figure 7: V850 anomalies in June-July-August for dry years (left panel) and wet years (right panel)

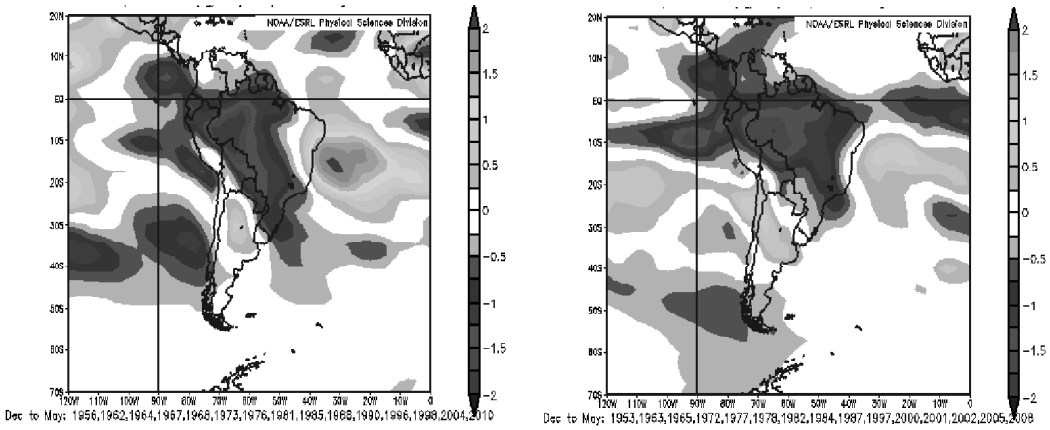

Figure 8: PW anomalies in summer and autumn (December to May) for dry years (left panel) and wet years (right panel)

SST composites clearly showed that positive (negative) phase of ENSO is associated with wet years (dry), especially in autumn, winter and spring. In spring the signal is high (Figure 9). In dry years, negative SST anomalies over Ecuador, are accompanied by a more intense South Pacific High (see positive anomaly near 30°S in G1000, Figure 3), divergence in the sea surface and upwelling are favored. In wet years, when the anticyclone is weakened (negative anomaly at 30°S in G1000, Figure 3), upwelling are weakened and positive SST anomalies are observed. No other significant differences in South Pacific SST are observed.

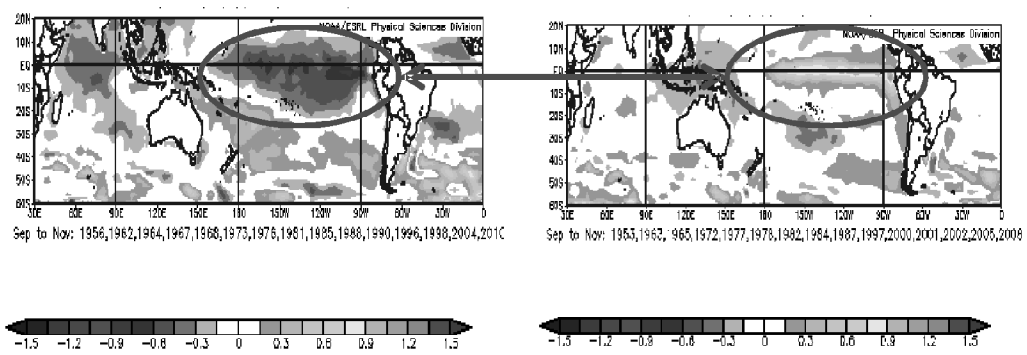

Figure 9: SST anomalies in September-October-November for dry years (left panel) and wet years (right panel)

3.2. Design of a regression model for predicting snow in central Andes (Argentina)

Previous results permitted to define some predictors, which were used to develop a statistical forecast model for predicting RAS, using two different techniques: Standard Multiple Regression (SMRM) and Forward Stepwise Regression Method (FSRM) (Wilks, 1995). SMRM derives an equation forcing some variables to act as predictors. FSRM chooses the best predictors and retains only those ones which best fit using a 95% significance level. FSRM is a model-building technique that finds subsets of predictor variables that most adequately predict responses on a dependent variable by linear regression, given the specified criteria for adequacy of model fit (Darlington, 1990). Basic procedures include both identifying an initial model, repeatedly altering it at the previous step by adding a predictor variable following a fixed criterion, and terminating the search when stepping is no longer possible as to the criteria. For both methods, predictors available to carry out the regression scheme were carefully selected, based on statistical significance, physical reasoning and independence of each other.

In order to apply the regression techniques, correlation field between RAS and oceanic and circulation variables were built. As it was desirable to predict snow in early June (just before winter), the predictors were defined using correlations between RAS and variables in May, April and March, in the period (March-April), (April-May) and (March-April-May). They are defined as the average variable over the area with maximum correlation. Variables selected were SST, G1000, G500, G300, U, V and PW from National Center of Environmental Prediction (NCEP) reanalysis (Kalnay *et al*, 1996). All variables were dimensionless:

$$VarA = \left(\frac{A - AMean}{AMean} \right) * 100 \qquad (1)$$

where *AMean* is the average of variable *A*. Table 3 shows all the predictors defined.

Table 3
Predictors defined based on the correlation fields between RAS and circulation and oceanic variables in previous periods. Predictors used to design the SMRM and FSRM were detailed and the correlation between the predictor an observed RAS serie is also detailed

Predictor Name	*Variable*	*Latitude Length*	*Periods*	*Correlation Coefficient with PRN*	*Method*
G1000	Pressure anomaly 1000 mb	50,0°S to 65,0°S 285,0°E to 305,0°E	April	0,35726053	MLRM SWM
		35,0°S to 40,0°S 290,0°E to 300,0°E	May	-0,3278901	
		35,0°S to 45,0°S 285,0°E to 300,0°E	April-May	-0,32283146	
		35,0°S to 45,0°S 280,0°E to 300,0°E	March-April-May	-0,32360552	MLRM
G500	Pressure Anomaly 500 mb	57,5°S to 70,0°S2 80,0°E to 305,0°E	April May	-0,36912384	
		35,0°S to 45,0°S 277,5°E to 292,5°E	April-May	-0,31152969	
		47,5°S to 67,5°S 277,5°E to 290,0°E		-0,23907358	
G300	Pressure anomaly 300 mb	60,0°S to 70,0°S 280,0°E to 300,0°E	April	-0,33910437	
		37,5°S to 47,5°S 280,0°E to 295,0°E	May	-0,25298021	
U850	Zonal wind anomaly 850 mb	37,5°S to 42,5°S 230,0°E to 260,0°E	May	-0,32315577	
SST–ENSO	Sea surface Temperature anomaly	4.8°N to 4.8°S 200.6°E to 270.0°E	April May	0,2578963 0,39133363	MLRM SWM
		4.8°N to 4.8°S 200.6°E to 270.0°E	April-May	0,33923006	
		4.8°N to 4.8°S 219,4°E to 270,0°E	March-April-May	0,2863817	
SST–SW Atlantic	Sea surface Temperature anomaly	31,4°S to 42,9°S 311,3°E to 333,8°E	April	0,34317842	
		29,5°S to 42,9°S 311,3°E to 330,0°E	May April-May	0,32968942 0,34794495	
			March-April-May	0,35857567	

contd. table 3

Predictor Name	*Variable*	*Latitude Length*	*Periods*	*Correlation Coefficient with PRN*	*Method*
SST–E Australia	Sea surface temperature anomaly	25,7°S to 37,1°S 159,4°E to 180,0°E	April	-0,32269129	MLRM SWM
		21,9°S to 37,1°S 159,4°E to 180,0°E	May	-0,29246322	
		25,7°S to 33,3°S 159,4°E to 185,6°E	April-May	-0,28113959	
		21,9°S to 37,1°S 159,4°E to 189,4°E	March-April-May	-0,29397486	
SST–SE Pacific	Sea surface Temperature anomaly	44.8°S to 54.3°S 260.6°E to 285.0°E	April	-0,20754755	
			May	-0,27725573	
			April-May	-0,17803178	
			March-April-May	-0,28098513	

Four predictors mainly correlated to rainfall and independent among each other were selected for the SMRM and they are detailed in Table 3. Figure 10 shows the correlation fields used to define the predictors. The entrance predictors were: G500 in April, SST(ENSO) in May, SST(East Australia) in April and G1000(Patagonia) averaged in March-April.-May. The equation of the standard linear regression forecast model was formulated as follows:

$$RAS = 97{,}8327873 - 2{,}8937922 * G500 + 6{,}8230141 * SST\,(ENSO) - 5{,}97177858 * SST\,(EAustralia) - 0{,}37626663 * G1000 \quad (2)$$

This model explained the 36,2% of the variance of RAS and showed that RAS is greater when G500 negative anomalies in April in middle levels are positioned south of Argentina as it can be noted in Figure 10a; when negative G1000 anomalies in the period March-April-May in low levels are detected over the area of study (Figure 10d); in warm phase of ENSO in May (Figure 10b)and when there are negative SST anomalies in East of Australia in April (Figure 10c). Figure 11 shows the observed RAS (red line), RAS predicted with SMRM (green line) and RAS derived from the crossvalidation method (blue line). A crossvalidation method was employed in which out of 60 years, 59 are used for calibration and the process is repeated 60 times. This approach is more robust in the presence of a long-term climate variability, which should show up as a gradual drift in the regression parameters. As four predictors were entered to the model and the model was constructed for 60 years, it was not a case of overfitting the data, and as the model remains similar, there was no evidence of numerical instability. Correlation between observed RAS and RAS derived from crossvalidation is 0,36 which resulted significant with 95% confidence

level. Figure 12 shows the relative percentage error between forecast RAS with SMRM and observed RAS, defined as the ratio between difference (observed RAS – predicted RAS) and observed RAS. It can be notice that the error is less than 50% in all wet years but is much higher in dry years.

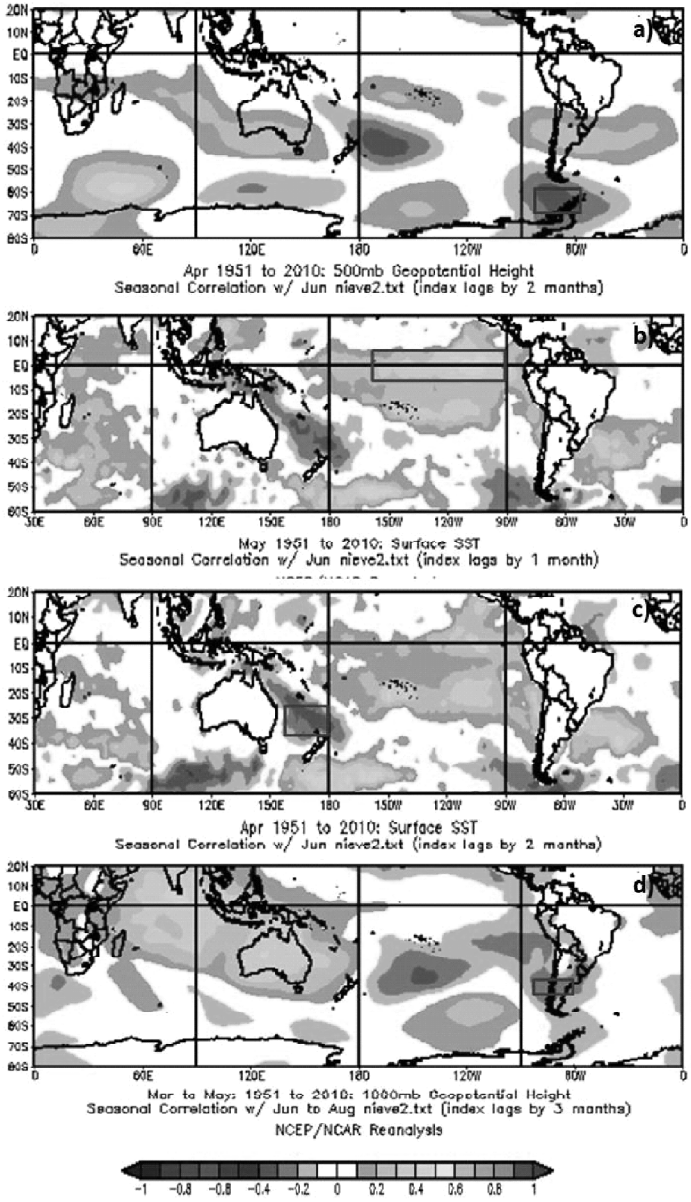

Figure 10: Correlation between RAS and G500 in April (a), SST(ENSO) in May (b), SST(East Australia) in April (c) and G1000(Patagonia) in March-April.-May (d)used to define predictors used in both models (SMRM and FSRM) which are remark in the figure

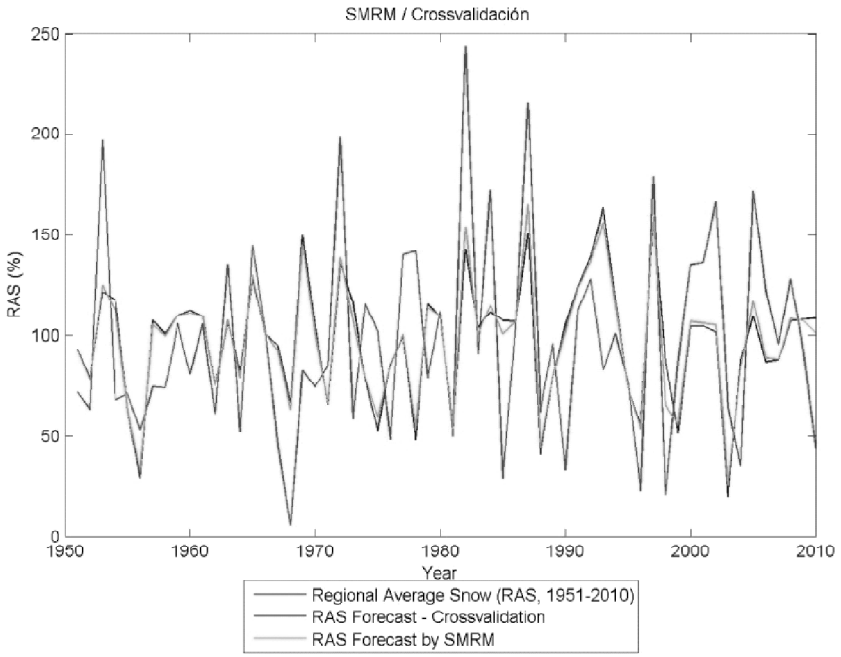

Figure 11: Observed RAS (red line), Predicted RAS with SMRM derived from equation (2) (green line) and RAS derived from crossvalidation of SMRM (blue line)

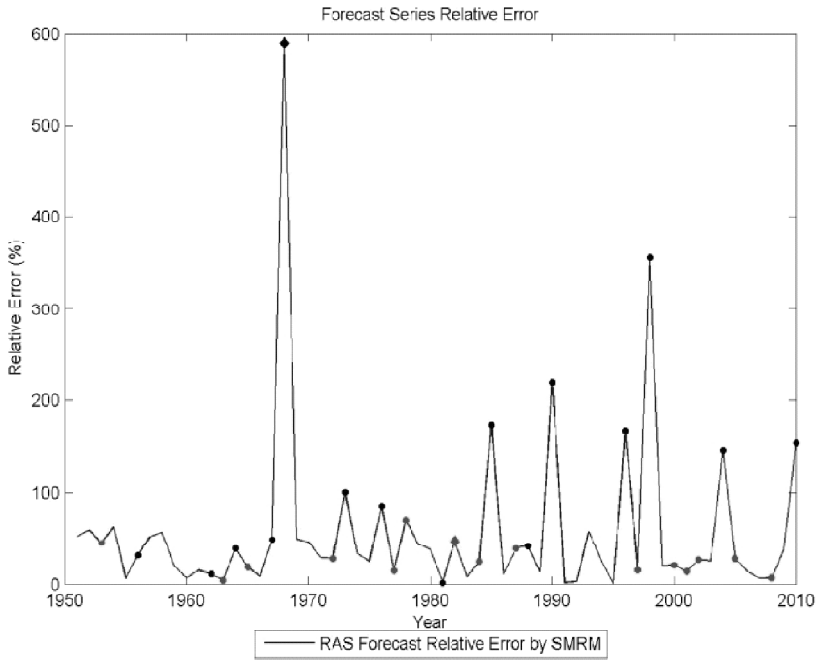

Figure 12: Forecast Series Relative Error for SMRM (blue). Dry years in black dots, wet years in red dots, driest year (1968) in black diamond and wetter year (1982) in red diamond

All monthly predictors detailed in Table 3, mainly correlated to rainfall and independent among each other, were selected to enter in FSRM. The model retained only the variables correlated with 95% significance level and they were: G500 in April, SST(ENSO) in May, SST(East Australia) in April. Note that they are three of the four variables used in SMRM. The equation of the linear regression forecast model was formulated as follows:

$$RAS = 97{,}9048 - 23{,}0189434 * G500 + 7{,}3582099 * SST\,(\text{ENSO}) - 6{,}82153176 * SST\,(EAustralia) \quad (3)$$

As in the case of SMRM, this model reflects the importance of SST in ENSO area and in eastern Australia and the geopotential anomalies in over and southern Argentina, in producing snow in Central Andes. The regression model explained the 19,3% of RAS variance. As the model remained similar when the crossvalidation method was applied, there was no evidence of numerical instability. Figure 13 shows observed RAS, RAS predicted with FSRM and the RAS resulted from the crossvalidation. The correlation coefficient between observed RAS and RAS from crossvalidation is 0,35, significant at 95% confidence level. Figure 14 shows the relative percentage error between forecast RAS with FSRM and observed RAS and, as in the case of SMRM, the error is substantially lower in wet years than in dry ones.

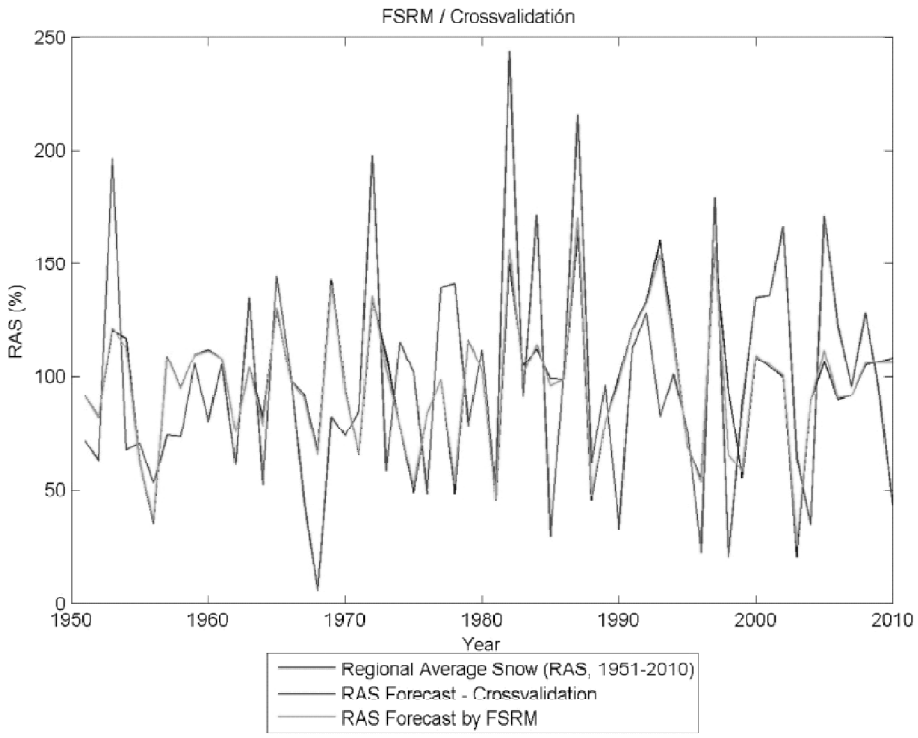

Figure 13: Observed RAS (red line), Predicted RAS with FSRM derived from equation (2) (green line) and RAS derived from crossvalidation of FSRM (blue line)

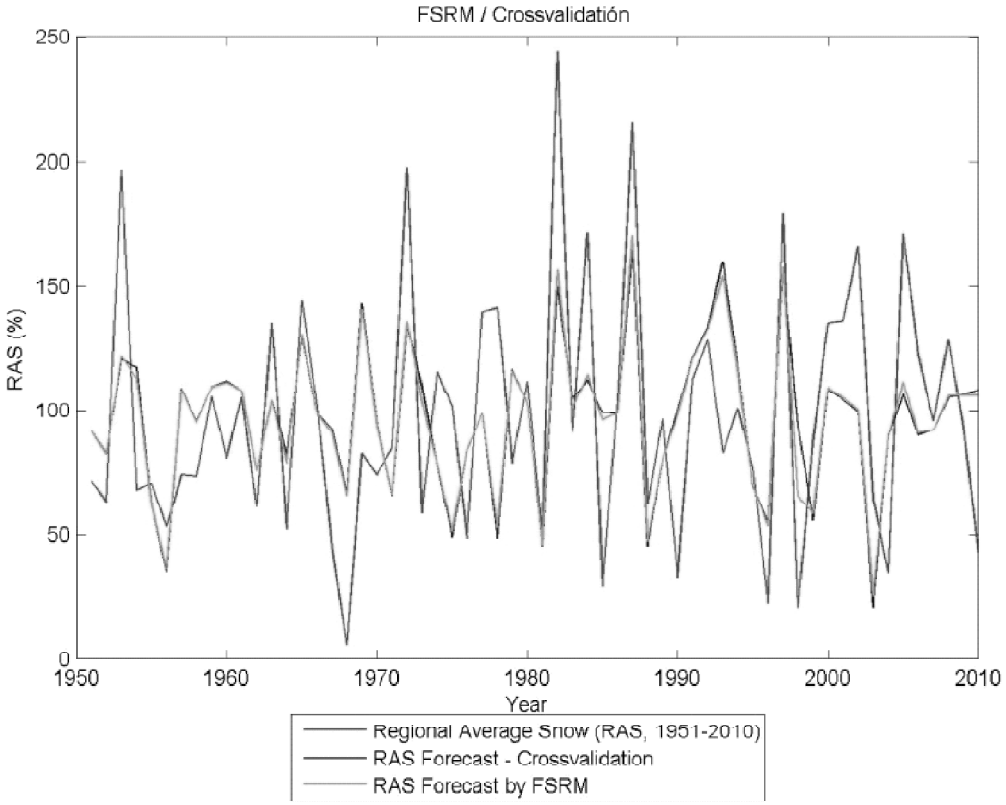

Figure 14: Forecast Series Relative Error for FSRM (blue). Dry years in black dots, wet years in red dots, driest year (1968) in black diamond and wetter year (1982) in red diamond

4. A CASE STUDY

Finally we considered the driest year (1968) and the wettest (1982) to analyze the variables mentioned, by way of case studies. Years 1968 and 1982 are the most extreme of the series, with a value of RAS 243.7% and 5.6% of the average values, respectively. For 1982, considered the wettest year of the series, the value associated RAS is larger than the third quartile and away +2.9 standard deviations from the mean. 1968, considered the driest year, RAS is lower than the first quartile and is at -1.81 standard deviations from the mean.

A clear opposite behavior between both (1982 and 1968), wet and dry years and similar to the behavior observed in the groups to which they belong is observed in G1000 composite (Figure 15), especially in winter. Negative G1000 anomalies are observed in 1968 near the Drake Passage in winter, meanwhile positive anomalies are present in 1982. In addition, negative anomalies over the South Pacific are also observed, showing a weakening of the systems in 1982.

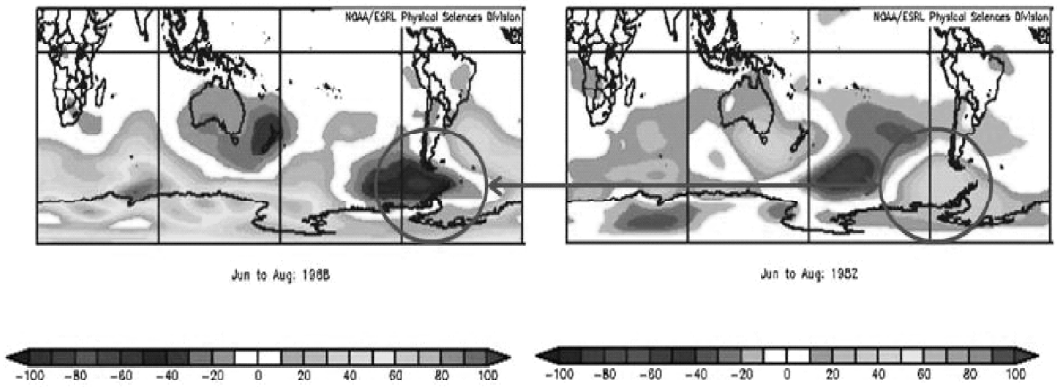

Figure 15: G1000 anomalies in June-July-August for 1968 (left panel) and 1982 (right panel)

A weakening of the westerlies around 60°S and intensification of the westerlies north of 60°S, are observed in U composite (Figure 16) in autumn and winter in 1968. The opposite pattern is present in 1982. Both year patters are similar in spring and summer (figures not shown).

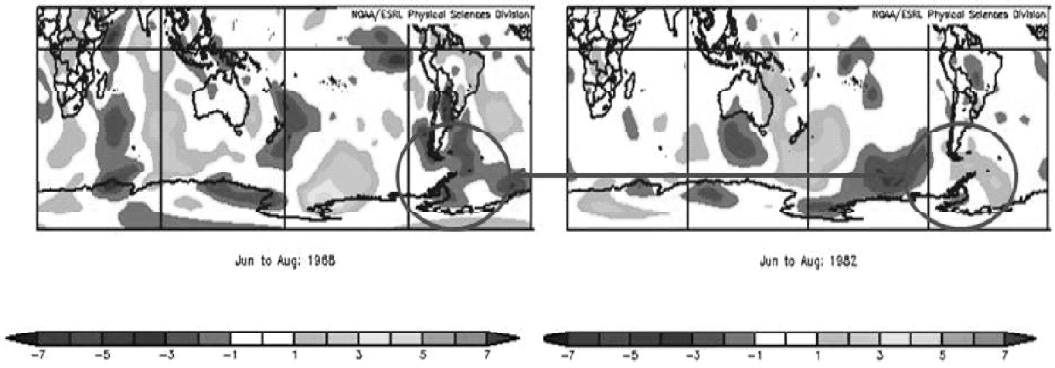

Figure 16: G850 anomalies in June-July-August for 1968 (left panel) and 1982 (right panel)

Looking at the evolution of the SST, we can detect the warm (cold) phase of ENSO present in 1982 (1968). According to the classification used, 1982 was a Niño year meanwhile 1968 was not a Niña year but high negative SST anomalies were present in tropical Pacific, as can be seen in the summer field (Figure 17).

In brief, there were two factors that were reinforced in 1982 and caused snow higher than normal: first the weakening of subpolar low and subtropical high in the eastern South Pacific and the other the event of the warm phase of ENSO. By contrast, 1968 was a year with little or no snow in Los Andes Mountain, associated with negative SST anomalies in the tropical Pacific and strengthening of the zonal circulation in the Pacific.

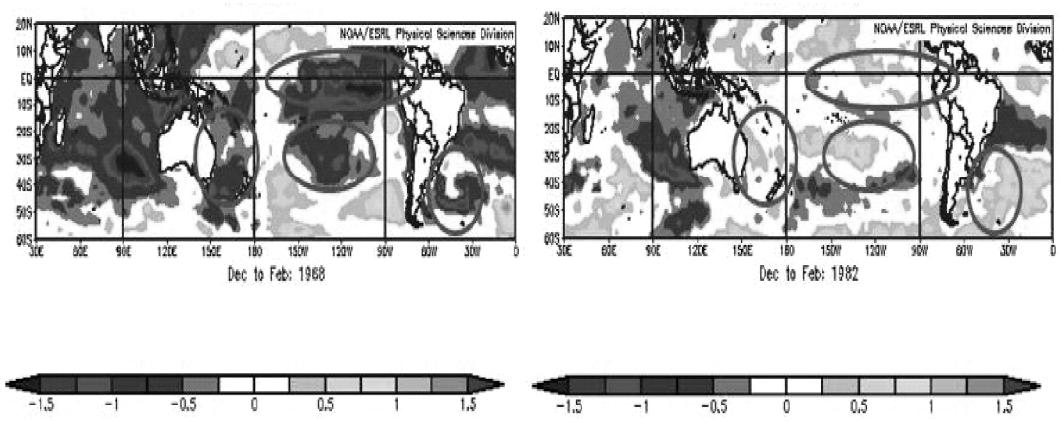

Figure 17: SST anomalies in June-July-August for 1968 (left panel) and 1982 (right panel)

5. CONCLUSIONS

According to analysis, different atmospheric patterns between wet and dry years, associated with snow excess or deficit in the Central Andes, could be detected. Wet years were associated with the weakening of both high and low pressure in the South Pacific, and thus a weakening of zonal flow, which facilitates the entry of frontal systems from the southwest to the mainland. Also, wet years were related to warm phase of ENSO. Possible predictors could be defined and a linear regression model was built to estimate the quantity of accumulated snow in winter and spring. Two approaches were used for prediction: a standard lineal multiple regression and a forward stepwise linear method. They both show the influence of mentioned factors over snow in Central Andes in Argentina and they both are efficient in predicting wet years but they fail to predict dry ones.

Acknowledgements

We thank Ricardo Villalba (IANIGLA, CCT Mendoza CONICET) for the support and the General Department of Irrigation of Mendoza, Argentina and General Water of Chile for collecting and supplying the snow data used in this study. The images of the figures of composite fields were provided by NOAA / ESRL Physical Sciences Division, Boulder Colorado from their website: http://www.esrl.noaa.gov/psd. This work was funded by the projects: UBACyT 2013-2016 20620120100003BA UBACyT 2014-20017 20020130100133BA.

References

[1] Aceituno, P. (1988). “On the functioning of the Southern Oscillation in the South American sector. Part I: surface climate”. Monthly Weather Review, 116, 505-524.

[2] Aceituno, P. and Garreaud, R. (1995). “Impactos de los fenómenos El Niño y La Niña sobre regímenes fluviométricos andinos”. Rev Soc Chilena Ing Hidráulica, 10(2), 33-43.

[3] Araneo, D. C. (2006). “Características de la Circulación Atmosférica y la Temperatura Superficial del Mar asociadas a extremos de caudal de ríos andinos y su variabilidad en baja frecuencia”. Tesis Doctoral. Facultad de Cs. Exactas y Naturales, UBA. 195 pp.

[4] Araneo, D. C. and Compagnucci, R. H. (2008). "Atmospheric circulation features associated to Argentinean Andean rivers discharge variability". Geophys. Res. Lett., 35, 1–6. doi:10.1029/2007GL032427.

[5] Aravena, J. C. and Luckman, B. H. (2008). "Spatio-temporal rainfall patters in Southern South America". Int J Climatol DOI: 10.1002/joc 1761.

[6] Barnston, A., Kumar, A., Goddard, L. and Hoerling, M. (2005). "Improving seasonal prediction practices through attribution of climate variability". BAMS, 59-72.

[7] Barros, V., Doyle, M., González, M., Camilloni, I., Bejarán, R. and Caffera, M. (2002). "Revision of the south american monsoon system and climate in subtropical south america south of 20°S". Meteorologica, 27, 33-58.

[8] Chan, S., Behera, S. K. and Yamagata, T. (2008). "Indian Ocean Dipole influence on South American rainfall". Geophysical Research Letters, 35, 14. L14S12 DOI: 10.1029/2008GL034204.

[9] Coelho, C., Stephenson, D., Balmaseda, M, Doblas Reyes, F. and Oldenborge, G. (2005). "Towards an integrated seasonal forecasting system for South America". J. Climate, 19, 3704-3721.

[10] Compagnucci, R. and Araneo, D. (2005). "Identificación de áreas de homogeneidad estadística para los caudales de los ríos andinos argentinos y su relación con la circulación atmosférica y la temperatura superficial del mar". Meteorologica, 30 1 and 2, 41-54.

[11] Compagnucci, R., and Blanco, S. (2000). "Variability in subtropical Andean Argentinean Atuel river; a wavelet approach". Environmetrics, 11, 251–269.

[12] Compagnucci, R. and Vargas, W. (1998). "Inter-annual variability of the Cuyo river streamflowin the Argentinean Andean Mountains and ENSO events". Int J Climatol., 18, 1593-1609.

[13] Darlington R. B. (1990). "Regression and linear models". McGraw-Hill. New York. 542 pp.

[14] Gillett, N. P., Kell, T. D. and Jones, P. D. (2006). "Regional climate impacts of the Southern Annular Mode". Geophysical Research Letters 33, L23704

[15] Gissila, T, Black, E., Grime, D. I. F. and Slingo, J. M. (2004). "Seasonal forecasting of the Ethiopian summer rains". Int. J. Climatol., 24, 1345-1358.

[16] Goddard, L., Barnston, A. and Mason, S. (2003). "Evaluation of the IRI´s "net assesment" seasonal climate forecasts 1997-2001". BAMS, 1761-1781.

[17] González, M. H. (2013). "Some indicators of interannual rainfall variability in Patagonia (Argentine)". Chapter 6 in Climate Variability Regional and Thematic Patterns, Editor: Dr. Aondover Tarhule. ISBN 980 9-533078-16 3. INTECH, UK.

[18] González, M. H. and Cariaga, M. L. (2011). "Estimating winter and spring rainfall in the Comahue Region (Argentine) using statistical techniques". Advances in Environmental Research, 11, 103-118.

[19] González, M. H. and Dominguez, D. (2012). "Statistical Prediction of wet and dry periods in the Comahue Region (Argentina)". Atmospheric and Climate Sciences, Doi: 10.4236/acs.2011, Publicación online http:www.scirp.org/journal/acs, Editorial: Scientific Research. Irvine, USA, 2, 1.

[20] González, M. H. and Flores, O. (2008). "La posible incidencia de los océanos en la precipitación en los Andes Centrales de Argentina". II Congreso Internacional sobre Gestión y Tratamiento Integral del Agua, PRODTI y Universidad de Córdoba, Córdoba, Argentina, 8188-197.

[21] González, M. H. and Herrera, N. (2014). "Statistical prediction of Winter rainfall in Patagonia (Argentina)". Horizons in Earth Science Research. Volume 11, Chapter 7. 221-238. Editor: Benjamin Veress and Jozsi Szigethy, NOVA Publisher, NY, USA.

[22] González, M. H.; Skansi, M. M. and Losano, F. (2010). "A statistical study of seasonal winter rainfall prediction in the Comahue region (Argentine)". ATMOSFERA, 23 (3), 277-294.

[23] González, M. H. and Vera, C. S. (2010). "On the interannual winter rainfall variability in Southern Andes". Int J Climatol, 30, 643-657.

[24] Grimm, A., Barros, V. and Doyle, M. (2002). "Climate variability in Southern South America associated with El Niño and La Niña events". J. Climate. 13-35.

[25] Kalnay, E., Kanamitsu, M., Kistler, R., Collins, W., Deaven, D., Gandin, L., Iredell, M., Saha, S., White, G., Woollen, J., Zhu, I., Chelliah, M., Ebisuzaki, W., Higgings, W., Janowiak, J., Mo, K. C., Ropelewski, C., Wang, J., Leetmaa, A., Reynolds, R., Jenne, R. and Joseph, D. (1996). "The NCEP/ NCAR Reanalysis 40 years- project". Bull. Amer. Meteor. Soc., 77, 3, 437-471.

[26] Kidson, J. (1999). "Principal modes of southern hemisphere low frequency variability obtained from NCEP-NCAR reanalyses". J. Climate, 12, 9, 2808-2830.

[27] Kumar, A. (2006). "On the interpretation and utility of skill information for seasonal climate predictions". Mon.Wea.Rev, 135, 1974-1984.

[28] Lenters, J. D. and Cook, K. H. (1995). "Simulation and Diagnosis of the Regional Summertime Precipitation Climatology of South America". Journal of Climate, 8, 12, 2988-3005.

[29] Masiokas, M. H., Villalba, R., Luckman, B. H., Le Quesne, C. and Aravena, J. C. (2006). "Snowpack Variations in the Central Andes of Argentina and Chile, 1951-2005: Large-Scale Atmospheric Influences And Implications for Water Resources in the Region". J. Climate, 19, 24, 6334–6352.

[30] Masiokas, M. H., Villalba, R., Luckman, B. H. and Mauget, S. (2010). "Intra-Multidecal Variations of Snowpack and Streamflow Records in the Andes of Chile and Argentina between 30º and 37ºS". J. Hydrometeorology, 11, 3, 822-831.

[31] Mitchell, J. M., Dzerdzeevsku, B., Flohn, H., Lamb, H. H., Rao, K. N. and Wallín C. C. (1971). "Technical Note Nº 79. Climatic Change (Report of a working group of the Comission for Climatology)". WMO, 195, 79.

[32] Montecinos, A. and Aceituno, P. (2003). "Seasonality of the ENSO related rainfall variability in Central Chile and associated circulation anomalies". J Climate, 16, 281-296.

[33] Nogues Paegle J. and Mo, K. C. (2002). "Linkages between Summer Rainfall Variability over South America and Sea Surface Temperature Anomalies". J. Climate, 15, 12, 1389-1407.

[34] Quan, X., Hoerling, M., Whitaker, J., Bates, G. and Xu, T. (2006). "Diagnosing source of US Seasonal forecast skill". J.Climate, 19, 3279-3293.

[35] Reason, C and Rouault, M. (2005). "Links between the Antartic Oscillation and winter rainfall over western South Africa". Geophys Res Lett., 32

[36] Reason, C. (2001). "Subtropical Indian Ocean SST dipole events and Southern Africa rainfall". Geophys Res Lett., 28, 2225-2227.

[37] Reboita, M. S., Ambrizzi, T. and Da Rocha, R. (2009). "Relationship between the Southern Annular Mode and Southers Hemisphere atmospheric systems". Revista Brasilera de Meteorologia; 24, 1, 48-55.

[38] Ropelewski, C., and Halpert, M. (1987). "Global and Regional scale precipitation patterns associated with El Niño". Mon Wea Rev, 115, 8, 1606-1626.

[39] Rutland, J. and Fuenzalida, H. (1991). "Synoptic aspects of the central Chile rainfall variability associated with the Southern Oscillation". Int J Climatol., 11, 63-76.

[40] Saji, N.H., Yamagata, T., Ashok, K. and Guan, Z. (2004). 2Individual and Combined Influences of ENSO and the Indian Ocean Dipole on the Indian Summer Monsoon". Journal of Climate, 17, 16, 3141-3155.

[41] Scarpati, O. E., Kruse, E., Gonzalez, M. H., Ismael, A., Vich, J., Capriolo, A. and Caffera, R. M. (2014). "Updating the hydrological knowledge: a case of study". Handbook of Engineering Hydrology, Vol. 3, Chapter 23: Environmental Hydrology and River Management. Editor: Prof Saeid Eslamian, Taylor & Francis. 443-457.

[42] Schneider, C. and Gies, D. (2004). "Effects of El Niño-Southern Oscillation on southernmost South America precipitation al 53ºS revealed from NCEP-NCAR reanalysis and weather station data". Int J Climatol., 24, 9, 1057-1076.

[43] Silvestri, G and Vera, C. (2003). "Antarctic Oscillation signal on precipitation anomalies over southeastern South America". Geophys Res Lett., 30, 21, 21-15.

[44] Singhrattna, N., Rajagopalan, B., Clark, M. and Krishna Kumar, K. (2005). "Seasonal Forecasting of Thailand summer monsoon rainfall". Int J of Climatol., 25, 649-664.

[45] Thompson, D.W. and Wallace, J. M. (2000). "Annular modes in the extratropical circulation. Part I: Month-to-month variability". J. Climate, 13, 1000-1016.

[46] Vera, C., Higgins, W., Amador, J., Ambrizzi, T., Garreaud, R., Gochis, D., Gutzler, D., Lettenmaier, D., Marengo, J., Mechoso, C. R., Nogues Paegle, J., Silva Dias, P. L. and Zhang, C. (2006). "Toward a unified view of the American Monsoon Systems". J. Climate. 19, 20, 4977-5000.

[47] Wang, M. and Paegle, J. (1996): "Impact of analysis uncertainty upon regional atmospheric moisture flux". J. Geophys. Res., 101, 7291 – 7303.

[48] Wilks, D.S. (1995). "Statistical methods in the atmospheric sciences (An introduction)". International Geophysics series. Academic Press, San Diego, California, USA, 467 pp.

[49] Zheng, X. and Frederiksen, C. (2006). "A study of predictable patterns for seasonal forecasting of New Zeland rainfall". J Climate, 19, 3320-3333.

[50] Zareian, M. J. and Eslamian, S., 2016, Variation of water resources indices in changing climate, International Journal of Hydrology Science and Technology, Vol. 6, No. 2, 173 – 187.